Femtosecond time-resolved laser-induced breakdown spectroscopy for detection and identification of bacteria: A comparison to the nanosecond regime

Matthieu Baudelet, Laurent Guyon, Jin Yu,[a] and Jean-Pierre Wolf
Laboratoire de Spectrométrie Ionique et Moléculaire, UMR CNRS 5579, Université Claude Bernard-Lyon 1, 43, Boulevard du 11 Novembre 1918, F-69622 Villeurbanne Cedex, France

Tanguy Amodeo and Emeric Fréjafon
Institut National de l'Environnement Industriel et des Risques (INERIS), Parc technologique ALATA, BP2, 60550 Verneuil-en-Halatte

Patrick Laloi
Laboratoire de Microbiologie et Génétique, UMR CNRS 5122, Université Claude Bernard-Lyon 1, 43, Boulevard du 11 Novembre 1918, F-69622 Villeurbanne Cedex, France

(Received 19 September 2005; accepted 9 February 2006; published online 19 April 2006)

Bacterial samples (*Escherichia coli* and *Bacillus subtilis*) have been analyzed by laser-induced breakdown spectroscopy (LIBS) using femtosecond pulses. We compare the obtained spectra with those resulting from the classical nanosecond LIBS. Specific features of femtosecond LIBS have been demonstrated, very attractive for analyzing biological sample: (i) a lower plasma temperature leading to negligible nitrogen and oxygen emissions from excited ambient air and a better contrast in detection of trace mineral species; and (ii) a specific ablation regime that favors intramolecular bonds emission with respect to atomic emission. A precise kinetic study of molecular band head intensities allows distinguishing the contribution of native CN bonds released by the sample from that due to carbon recombination with atmospheric nitrogen. Furthermore a sensitive detection of trace mineral elements provide specific spectral signature of different bacteria. An example is given for the Gram test provided by different magnesium emissions from *Escherichia coli* and *Bacillus subtilis*. An entire spectrum consists of hundred resolved lines belonging to 13 atomic or molecular species, which provides an ensemble of valuable data to identify different bacteria. © *2006 American Institute of Physics*. [DOI: 10.1063/1.2187107]

I. INTRODUCTION

Detection and identification of microbiological samples such as bacteria, molds, or pollens has become a critical application for either military and civil defense or environmental surveillance. Large efforts have been dedicated to demonstrate and test methods that provide reliable, fast, and sometimes standoff detection of microbiological samples. Laser-induced breakdown spectroscopy (LIBS) has been considered as a promising method for laboratory or field detection and identification of microbiological samples in bulky or spread aerosols forms. Several works using nanosecond laser-induced breakdown spectroscopy (nano-LIBS) have been reported. These experiments have been designed for identifying spectral markers of microbiological samples and testing suitable spectral data processing methods to extract valuable information for distinguishing different species.[1–4] Detection of a single bioaerosol has also been demonstrated with nanosecond LIBS.[5–7] However, the potential of femtosecond laser-induced breakdown spectroscopy (femto-LIBS) for detection and analysis of biological samples has not been studied so far, although femto-LIBS has been successively demonstrated recently for inorganic matter detection with a number of attractive features.[8–10]

These interesting features of femto-LIBS are basically due to the specific ablation regime of femtosecond pulses. A pulse duration shorter than the thermal coupling time constant in matter (~1 ps) leads to a domination of multiphoton-induced ionization over thermal decomposition, and an expansion of the ejected plasma without further interaction with the laser pulse. The specific properties of femtosecond ablation have been extensively studied for better performance of laser micromachining or microfabrication.[11] Efficient, fast, and localized energy deposition in femtosecond regime allows minimum thermal and mechanical damage of the substrate and a precise material removal. For analysis purposes using LIBS, specific properties of the plasma induced by a femtosecond pulse, such as lower and faster decreasing temperature[12–14] and explosive ejection of matter,[15] allow us to expect an improved sensibility for trace element detection.

We already demonstrated that, in femto-LIBS detection of a metallic sample, emission from excited ambient air is practically negligible because of a lower temperature of the laser-induced plasma.[8–10] This contrasts with nano-LIBS, in which the air in vicinity of the laser impact spot emits an intense spectrum of atomic nitrogen and oxygen in the near infrared.[8,10] For the analysis of organic or biological materials, this air spectrum interferes with emission from the sample, especially in the region of the near infrared.[1] Lower

[a]Author to whom correspondence should be addressed; electronic mail: jin.yu@lasim.univ-lyon1.fr

temperature of femtosecond laser-induced plasma reduces drastically the blackbody emission from the plasma according to Stefan's law of fourth power temperature dependence of the radiation power. That allows plasma lines to be detected with a higher contrast (high line to continuum ratio),[16] which is crucial for detecting trace mineral elements in a biological sample. For organic as well as biological matter analysis, spectral signatures from molecular bonds are very important since radicals, such as CN or C_2, are characteristic of the biological medium. Neutral N_2 has been observed as the most abundant species released in nanosecond UV laser ablation of a polymer.[17] The mechanism that distinguishes nanosecond UV from nanosecond IR interaction with organic matter is that the multiphoton absorption in UV leads to ionization and decomposition through pathways that are different from thermal decomposition.[18,19] Multiphoton ionization ablation also occurs for ultrashort laser pulse interaction with organic or biological matters, which let us hope significant molecular fragments to be produced in femtosecond ablation. Femtosecond LIBS thus provides significant molecular spectral signatures of a sample together with the more usual atomic spectral signature, which allows a better characterization of the sample especially when an organic or a biological medium is studied.

In this paper we describe the experimental setup and the results of our experiments designed to demonstrate femto-LIBS analysis of bacteria. The LIBS spectra from bacteria using both femtosecond and nanosecond pulses are presented. We compare the LIBS spectra of these two pulse duration regimes in order to emphasize the attractive features of femto-LIBS for the analysis of biological samples. We especially show that a lower temperature in the femtosecond laser-induced plasma permits a higher contrast for the detection of trace elements in a bacterial sample. We observe an enhanced molecular band emission in femto-LIBS spectra. We also present a kinetic study of molecular bands, CN and C_2, which are very important for organic or biological sample analysis. We demonstrate that native intramolecular bonds can be ablated directly from a bacterial sample. Their spectral emission can be distinguished from that due to the molecular bonds formed during the expansion of a plasma plume by carbon recombination with ambient air. More precisely, different behaviors of the time evolution of the molecular band head are clearly observed corresponding to different origins of the molecular bonds. Based on our results we propose a general strategy to detect bacteria from a natural background and to further distinguish different species of bacteria.

II. EXPERIMENTAL SETUP

In our experiments (Fig. 1), we used either a Ti:sapphire femtosecond laser system or a Nd:YAG (yttrium-aluminum-garnet) nanosecond laser in order to have a comparison of these two pulse durations. The femtosecond laser consists of an oscillator, a regenerative amplifier and a multipass amplifier. The system provides 120 fs pulse at 810 nm with a 20 Hz repetition rate. Typical pulse energy used in our experiments is 4.5 mJ. The nanosecond laser provides pulses of

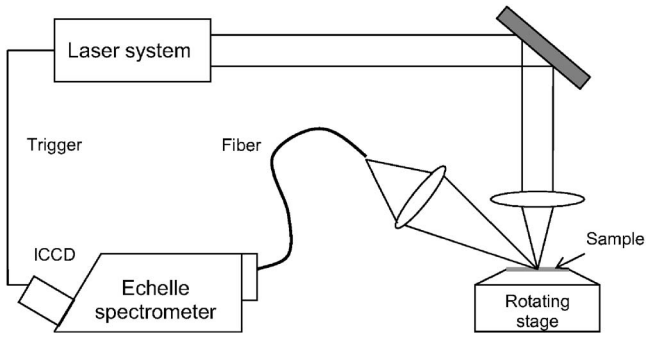

FIG. 1. Schematic presentation of the experimental setup.

5 ns duration at 1064 nm and a repetition rate of 20 Hz. The same pulse energy is used to compare with the femtosecond regime. The laser beam is focused on the surface of a sample using a single lens of 30 mm focal length. The resulting beam waist is about 100 μm, leading to a fluence of about 14 J/cm^2 for the both pulse duration regimes. To have a fresh spot for each laser shot, the sample is fixed on a rotation stage.

Bacterial samples of *Escherichia coli* (*E. coli*) and *Bacillus subtilis* (*B. subtilis*) are prepared according to the following procedure: growth of bacteria overnight in a nutrition medium (the same nutrition medium for both bacteria) at 37 °C under aeration; impact by aspiration of 20 mℓ solution of bacteria on a filter; washing of the charged filter by 20 mℓ distilled water with the same aspiration process; and drying for about an hour. Intuitively a metallic filter would be advantageous because it leads to a simpler background spectrum and less interference with the bacteria.[1] A trial with a silver filter (Millipore, catalog no. AG4502550) showed, however, an unsatisfactory result in the femtosecond regime, since two-photon-induced plasmon emission saturated the detection system in the spectral range around 400 nm. Cellulose nitrate membrane filters (Whatman, catalog no. 7184-004) have finally been preferred in our experiments. These filters have pores of 0.45 μm diameter, suitable to trap bacteria. Organic filters are moreover much less expansive than metallic filters and provide a more realistic analytical environment for applications. However, the use of an organic filter requires differential measurements. We recorded in the same experimental conditions, spectra of a filter charged with bacteria, a filter charged with the nutrition medium (same preparation procedure as for bacteria-charged filter without bacteria growth), and an unexposed filter. Only nonpathogenic agents were analyzed in this study, which avoided sophisticated protection system. The nutritional medium was liquid Luria Broth from Biomerieux. The resulting sample was a bacteria-charged filter of 4 cm diameter containing a layer of bacteria with a thickness of about 100 μm. Mechanic resistance of the samples against laser ablation was important to allow experiences to be carried out over hours. We stuck the samples on a Plexiglas plate to enhance its mechanic resistance.

Plasma emission was collimated by a single quartz lens with a focal length of 50 mm and a diameter of 25 mm. The optical axis of the collecting system was at about 45° from the laser axis. The position of the lens was set so that the

image of the laser-induced plasma was formed at the entrance of a coupling fiber (25 μm aperture) with a magnification of 0.4. This setup was not intended to have a spatially resolved observation of the plasma plume. However, a three-dimensional (3D) microdisplacement stage allowed a precise position of the fiber entrance on the part of the image that corresponded to the part of the plasma plume with the highest light emission (most likely very close to the impact point of laser pulses on the sample surface). The output end of the fiber was attached to the entrance slit (25×50 μm^2 aperture) of an Echelle spectrometer (focal length of 195 mm and f-number=7) equipped with an intensified charge-coupled device (ICCD) camera (Andor Technology, Mechelle and iStar). The ensemble of Echelle spectrometer and ICCD camera provided a spectral range from 200 to 920 nm, with a resolution of 0.04 nm at 200 nm and 0.2 nm at 1000 nm. A temporal window was set on the ICCD camera with high precision synchronized on each laser shot.

In our experiments two types of spectra were observed: Time-integrated spectra corresponding to a 5 μs detection window opened several hundreds nanosecond (typically 100 or 200 ns) after each laser shot; kinetic series, where the plasma emission was detected within a reduced detection window of 50 ns width, while the time delay of the detection window was scanned to get the study of time evolution of the emitted spectrum from the instant when laser pulse arrives on the sample. A minimum detection delay was necessary after each laser shot to avoid saturation of the camera by continuum emission from the plasma. This delay was shorter in the femtosecond regime than in the nanosecond regime due to a lower temperature of the femtosecond laser-induced plasma. For either time-integrated spectra or kinetic series, each spectrum was accumulated for 1000 laser shots.

III. EXPERIMENTAL RESULTS AND DISCUSSIONS

A. Time-integrated spectra: A comparison between femto- and nano-LIBS

Figure 2 shows time-integrated spectra of *E. coli* obtained with femtosecond pulses [Fig. 2(a)] and nanosecond pulses [Figs. 2(b) and 2(c)]. Look first at Figs. 2(a) and 2(b). Both of these spectra were recorded with a detection delay of 100 ns, a maximal gain for the ICCD camera (gain=255), and with detection windows of 5 μs and 50 ns for Figs. 2(a) and 2(b) respectively. In this overview presentation of the spectra, one can already observe differences between the two temporal regimes. Continuum emission is much more significant in the nanosecond spectrum than in the femtosecond spectrum. That can be clearly seen by comparing Figs. 2(a) and 2(b). For the same delay of 100 ns, continuum emission from the femtosecond pulse-induced plasma is already damped down enough to allow a good line to continuum ratio of the spectrum, while in the nanosecond regime the spectrum is still totally dominated by the continuum emission, which saturates the camera. Notice that the quasiperiodical modulation on the continuum spectrum is due to the spectral efficiency of the spectrometer. In order to avoid the saturation of the camera and get a good line to continuum ratio, in Fig. 2(c), a nanosecond spectrum is recoded with a

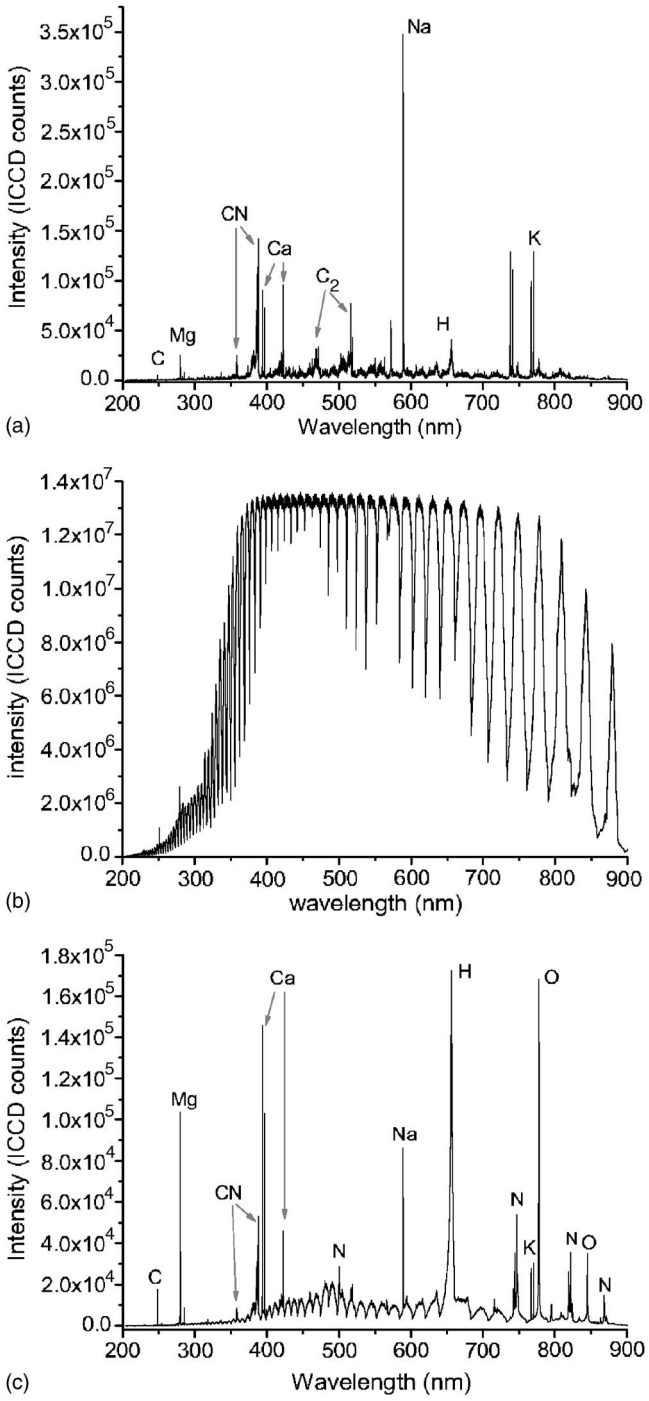

FIG. 2. Time-integrated spectra of *E. coli* with (a) femtosecond pulses and [(b) and (c)] nanosecond pulses.

detection delay of 200 ns, a detection window of 5 μs and a minimal ICCD gain (gain=0). These detection parameters provide a good quality nanosecond spectrum that we used in the rest of this section to give a detailed comparison between the tow temporal regimes. Since the continuum emission intensity is crucially related to plasma temperature ($\propto T^4$), the weak continuum emission in the femtosecond regime confirms a lower temperature in femtosecond laser-induced plasma averaged over the detection period.

An important consequence of lower plasma temperature in the femtosecond regime is that the emission from excited

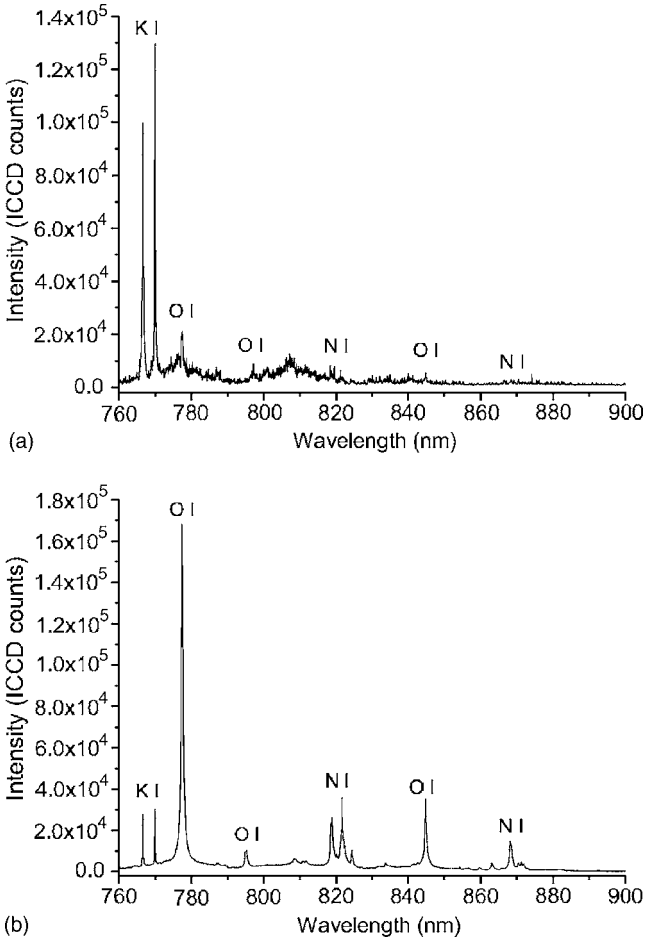

FIG. 3. Detailed spectra of *E. coli* in the near infrared in (a) femtosecond regime and (b) nanosecond regime.

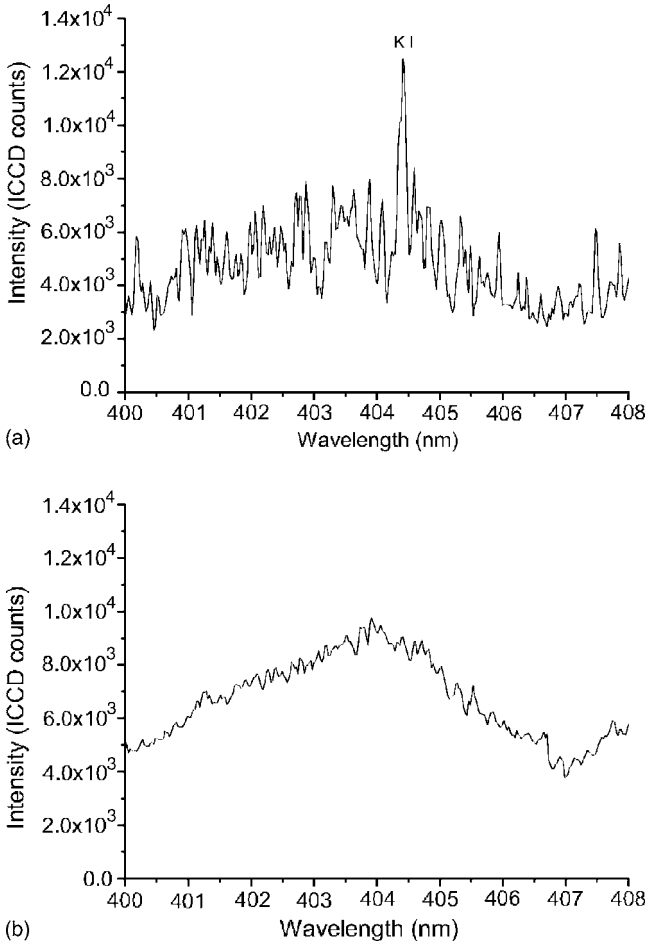

FIG. 4. Detailed spectra of *E. coli* with (a) femtosecond pulses and (b) nanosecond pulses showing the K I 404.41 line in the femtosecond spectrum.

ambient air (oxygen and nitrogen lines) is almost not observed in contrast with the nanosecond regime. In Fig. 3 detailed spectra are shown in the near infrared to illustrate the reduced ambient air emissions in the femtosecond regime as compared to the nanosecond regime. One can, for example, compare for both the temporal regimes, the intensities of line emissions from atomic nitrogen and oxygen to those of the two lines from potassium atoms. This result is consistent with our previous observations on a metallic target.[8,10] Such very low ambient air excitation in the femtosecond regime prevents ambiguities in interpretation of atomic nitrogen and oxygen lines, which can also be emitted by a biological sample.

Another important consequence of lower plasma temperature in the femtosecond regime is that trace mineral elements can be detected from bacteria with a higher contrast. The reason is the less intense and quickly damped continuum emission, allowing a shorter detection delay after each laser shot. As shown below, mineral atomic emitters have very short lifetimes (typically less than 100 ns). A short detection delay is thus crucial for their detection. Figure 4 shows detailed spectra from *Escherichia coli* obtained using femtosecond [Fig. 4(a)] and nanosecond [Fig. 4(b)] pulses. The very weak K I 404.41 nm line is perfectly resolved in the femtosecond spectrum, while it cannot be distinguished at all in the nanosecond spectrum. As shown in Fig. 5, other more intense mineral atomic lines, such as the 421.03 and 421.36 nm iron lines or the 422.67 nm calcium line, can be observed in both regimes but with a much better contrast and resolution using femtosecond excitation. As already known, trace mineral elements are very important and specific for micro-organisms such as bacteria, as they actively participate in their metabolism and have an influence on their structure.[20] The detection of the spectral signatures from mineral elements therefore provides valuable information to distinguish different bacteria.

An example of the correlation between mineral element emission in a LIBS spectrum and a biological property of a bacterial sample is given in Fig. 6 with emissions from neutral and ion magnesium. Emissions from Mg II 279.55 and 280.27 nm lines, and Mg I 285.17 nm line were detected in femto-LIBS spectra of both *E. coli* and *B. subtilis*, grown in an identical nutritional medium. Both spectra are averaged over five independent spectra accumulated each for 1000 laser shots. We see clearly that the emissions from magnesium are significantly larger in *E. coli* than in *B. subtilis*. The difference is much larger than the standard deviation calculated from the five independent spectra, which is 16% of the signals. The difference in magnesium concentration is related to the different structures of these two bacteria. It is known that *E. coli* is a Gram-negative bacterium, while *B. subtilis* is

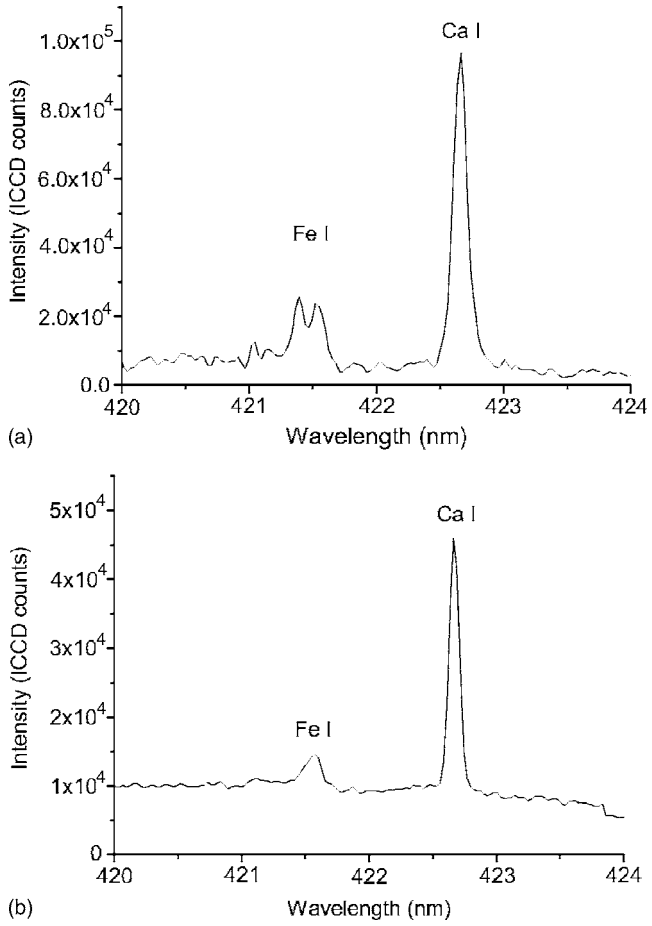

FIG. 5. Detailed spectra of *E. coli* with (a) femtosecond pulses and (b) nanosecond pulses showing 421.03 and 421.36 nm iron lines and 422.67 nm calcium line.

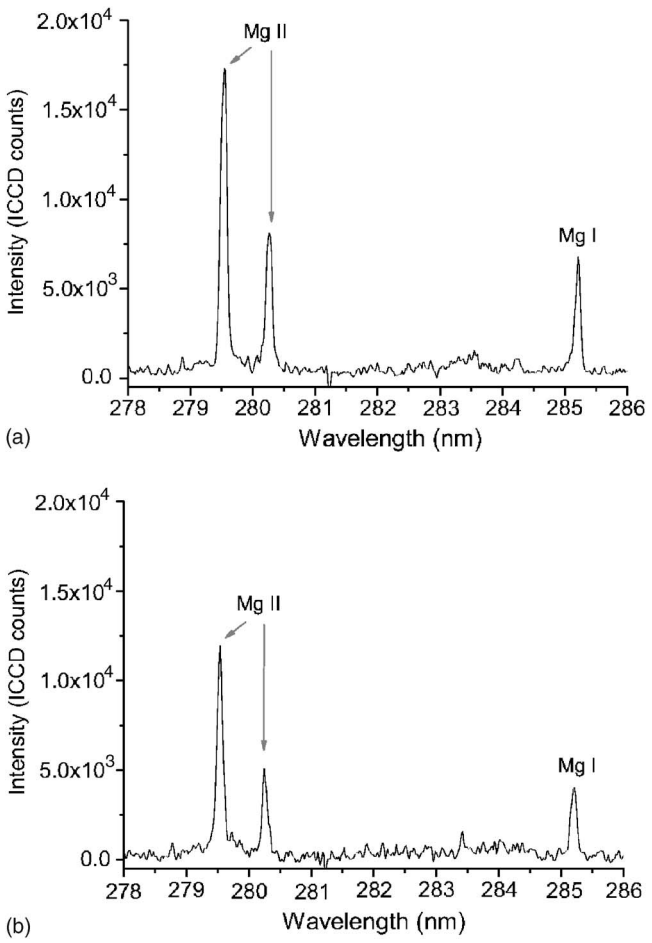

FIG. 6. Detailed femto-LIBS spectra (a) of an *E. coli* sample, and (b) of a *B. subtilis* sample showing a comparison of the emission intensities of Mg II 279.55 and 280.27 nm lines and Mg I 285.17 nm line. The spectra were recorded with same experimental conditions.

a Gram-positive one. A specific outer membrane envelops a Gram-negative bacterium. In this outer membrane, different proteins are maintained together by divalent cations, such as Mg^{+2} and Ca^{+2}. We expect thus find a more intense magnesium emission from a Gram-negative bacterium, such as *E. coli.* The intensity of magnesium emission measured from a LIBS spectrum of a bacterium is thus correlated to the classification of bacteria by the standard Gram test used in microbiology.[20]

A remarkable difference between femto- and nano-LIBS spectra consists also in the ratio between molecular and atomic emissions. For carbon, for example, the most abundant element in organic materials, we find very different intensity ratios of molecular bands to atomic line, CN/C or C_2/C, between a femtosecond spectrum and a nanosecond spectrum. These ratios are significantly larger in the femtosecond spectra than in the nanosecond spectra, as shown in Fig. 7 for the CN band compared to the C line and in Fig. 8 for the C_2 band compared to the C line. The larger molecular band to atomic line intensity ratio for femtosecond spectra implies that the ablation in the femtosecond regime produces more molecular species than in the nanosecond regime. This result is similar to previous observations in the nanosecond UV ablation of organic matters.[17–19]

This property of femto-LIBS is interesting for the analysis of organic and biological samples, since such samples are characterized by functional groups that consist of intramolecular bonds. For example, the CN bond is characteristic of the presence of the amino group, $–NH_2$, in a biological sample. The detection of CN bands in a LIBS spectrum may thus provide an indication (certainly not definitive) of a biological medium. However, it has been demonstrated that CN radicals can be formed when a laser-induced plasma expands through ambient air by carbon recombination with atmospheric nitrogen. Such recombination is observed either in nanosecond UV (Ref. 21) or nanosecond IR (Ref. 22) laser pulse-induced plasmas. The origins of the CN bands in a LIBS spectrum thus have to be carefully checked. We will show in the following section that with time-resolved femto-LIBS, it is possible to identify the contribution of native CN bonds released by the sample, which might provide a signature of a biological medium.

A detailed analysis of spectra from *E. coli* obtained with both femtosecond and nanosecond LIBS is summarized in Table I. Atomic[23] and molecular[24] spectral data bases were used for spectral line identification. We precise for each resolved line the spectral position and the relative importance in the femtosecond and the nanosecond regimes. Some of the lines are almost only observed in the femtosecond regime, others almost only in the nanosecond regime (in these cases

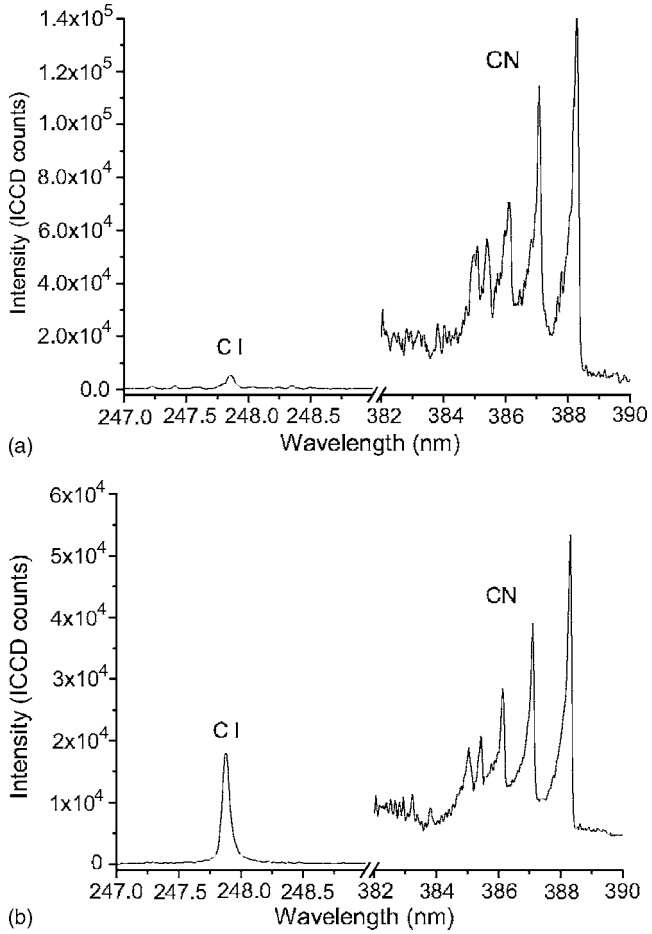

FIG. 7. Detailed spectra of *E. coli* with (a) femtosecond pulses and (b) nanosecond pulses showing 247.86 nm carbon atomic line and CN molecular band around 387 nm.

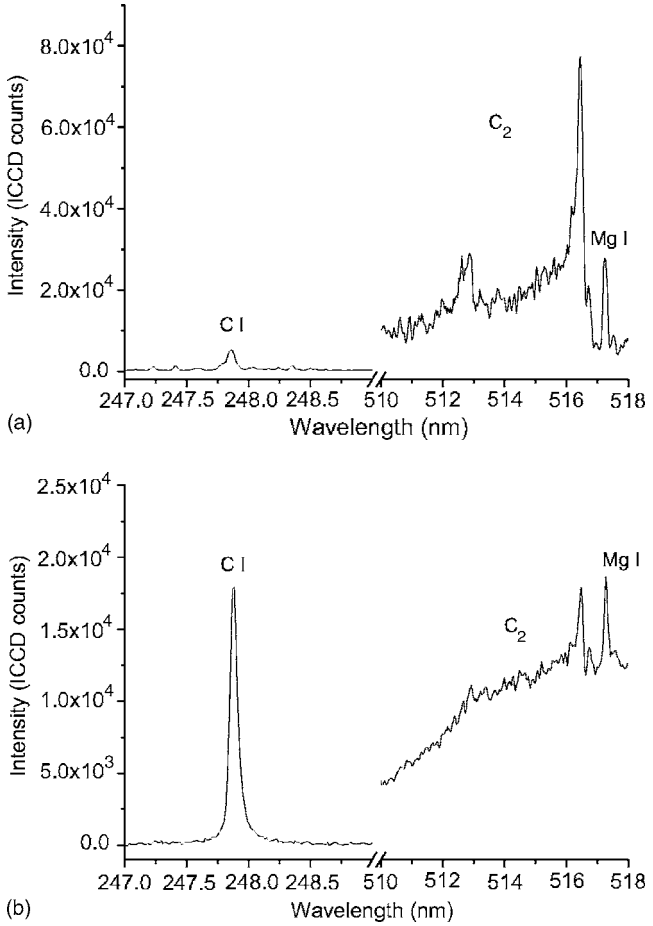

FIG. 8. Detailed spectra of *E. coli* with (a) femtosecond pulses and (b) nanosecond pulses showing 247.86 nm carbon atomic line and C_2 molecular band around 516 nm.

their intensity in the other temporal regime is almost in the noise level). Some of lines can be observed in the both regimes with comparable or quite different relative intensities. A specific line can also be observed in different sample: almost only in the bacteria; in the bacteria and in the nutritional medium; in the bacteria, in the nutritional medium and in the filter; or in the bacteria and in the filter. The specific spectral lines from the bacteria are easily identified in this way by simple differentiation. Globally hundred of lines are resolved, and can be attributed to 13 different atomic or molecular emitters.

B. Time evolution of the spectral emissions from femtosecond laser-induced plasma

After each laser shot the induced plasma emits a characteristic spectrum which evolves in time. Different emitters, atoms, or molecular bonds, have their specific decay time constants. The determination of these time constants has practical interest for precisely setting the time detection window in a synchronized detection. For molecular species, kinetic study has a fundamental interest, because as mentioned above molecular bonds can either be released directly from the sample or formed by recombination with ambient air. Only a time-resolved study allows a distinction between native intramolecular bonds ablated from the sample and molecular bonds formed by recombination.

Figure 9 shows the time evolution of the intense Ca I 422.6 nm line. The emission quickly decays between 50 and 100 ns. The relative uncertainty due the fluctuation from one kinetic series to other was estimated to be ±10%. A fit with exponential decay functions (experimental uncertainties taken into account) yields a decay time constant of (60±15) ns. Other less intense mineral lines exhibit similar decay time constants. Shortness of the lifetime of mineral atomic emissions explains the importance of a low plasma temperature for their detection with a high contrast.

Concerning the molecular bands observed in the spectra, it has been demonstrated that CN bonds can be formed by the reaction $C_2+N_2 \leftrightarrow 2CN$ when a graphite sample is ablated by UV or IR nanosecond laser pulses (KrF at 248 nm or Nd:YAG at 1064 nm) in ambient air containing nitrogen.[21,22] The time constant of recombination in a UV nanosecond laser-induced plasma is several hundreds of nanoseconds, during which the molecular band head intensity increases to a maximum value before it decays to zero.[21] This time evolution can be perfectly resolved with our detection system. In contrast, the contribution of native CN bonds released by a biological sample would monotonically decay from a maximum value to zero. To get representative con-

TABLE I. Resolved spectral lines in time-integrated spectra obtained in the both femtosecond and nanosecond regimes of *E. coli* and identified atomic and molecular species. Relative importance of the lines in femtosecond or nanosecond regimes is specified in the column "Temporal regimes." Observation conditions relative to samples are specified in the column NB. The following labels are used to precise the observation condition of a spectral line: F!: almost only observed in femto-LIBS; F: intense in femtosecond regime, weaker in nanosecond regime; F/N: observed in femto-LIBS as well as in nano-LIBS with comparable relative intensity; N: intense in nanosecond regime, weaker in femtosecond regime N!: almost only observed in nano-LIBS. For different types of samples, a specific spectral line can be observed either: (1) almost only in bacteria (NB: 1) (2) in bacteria and in nutritional medium (NB: 2), (3) in bacteria, in nutritional medium and in filter (NB: 3), or (4) in bacteria and in filter (NB: 4).

λ (nm)	Species	Temp. regime	NB	λ (nm)	Species	Temp. regime	NB	λ (nm)	Species	Temp. regime	NB	λ (nm)	Species	Temp. regime	NB
247.86	C I	F/N	3	416.70	CN	F	3	516.45	C2	F!	3	748.62	NI	F!	3
279.54	Mg II	F/N	2	418.07	CN	F	3	516.71	Mg I	F	1	766.55	KI	F	3
280.28	Mg II	F/N	2	419.65	CN	F	3	517.23	Mg I	F	1	769.92	KI	F	3
283.43	⋯	F!	1	421.52	CN	F	3	518.37	Mg I	F!	1	777.47	OI	N	3
285.17	Mg I	F	2	421.05	Fe I	F!	1	550.10	Fe I	F!	1	795.26	OI	N!	3
313.18	Fe II	F!	1	421.39	Fe I	F!	1	558.46	C2	F	3	797.12	⋯	F!	1
313.43	Fe II	F!	1	422.66	Ca I	F	3	563.47	C2	F	3	818.37	Na I	F!	3
				426.24	⋯	F!	1	572.15	⋯	F!	2	818.86	NI	N	3
317.94	Ca II	F/N	1	430.28	Ca I	F	1	572.72	⋯	F!	2	819.44	Cl I	F!	3
336.00	O II	F	3	432.04	⋯	F!	1	574.37	⋯	F!	1	824.34	N I	N	3
358.26	CN	F/N	4	441.49	O II	N!	3	589.01	Na I	F	3	833.62	⋯	N!	3
358.34	CN	F	3	443.52	Fe I	F	1	589.59	Na I	F	3	844.73	O I	N	4
358.57	CN	F	3	444.70	N II	N!	3	607.18	⋯	F!	1	854.20	Ca II	N	3
358.99	CN	F	3	445.51	Na II	F!	4	625.94	⋯	F!	1	856.68	N II	N!	3
373.78	Fe I	F	1	459.90	Fe I	F!	1	635.59	⋯	F	3	859.63	⋯	N!	1
385.10	CN	F	3	462.63	P II	F!	1	656.08	H I	F/N	3	863.14	NI	N	3
385.39	CN	F	3					711.83	Fe I	F!	1	868.15	NI	N	3
386.13	CN	F	3	467.81	C2	F!	3					870.46	N I	N	3
387.08	CN	F	3	467.96	C2	F!	3	720.16	Ca I	F	4	871.28	N I	N!	3
387.80	Fe I	F!	1	468.46	C2	F!	3	738.30	⋯	F!	2	871.95	N I	N!	3
388.29	CN	F	3	469.71	C2	F!	3	741.36	⋯	F!	2	874.06	P I	F!	1
393.35	Ca II	F	3	471.45	C2	F!	3	742.44	N I	N!	3	881.93	O I	N!	3
396.83	Ca II	F	3	473.65	C2	F!	3	744.33	N I	N!	3				
404.42	K I	F!	1	500.58	N II	N!	3	746.94	N I	N!	3				
415.74	CN	F	3	512.87	C2	F!	3	747.35	Fe I	F!	1				

figurations with respect to nitrogen and carbon containing in inorganic as well organic matter, we used three samples for this kinetic study: graphite, which contains exclusively carbon rings; cellulose nitrate membrane filter, where nitrogen atoms are provided by the nitrate group $-ONO_2$ and where CN bonds do not exist initially; and bacterial samples, *E. coli* and *B. subtilis*, where native CN bonds is a characteristic intramolecular bond provided by the connection of amino groups $-NH_2$ or =NH to carbon atoms.

Time-integrated spectra show similar CN and C_2 bands for the four samples even if the intensity ratio C_2/CN is higher for the graphite sample. Thus CN bands in a time-integrated spectrum do not represent a significant marker of CN intramolecular bonds in a sample. This is consistent with the conclusion from previous works on the nanosecond LIBS analysis of bacteria.[1,2] Kinetic study is thus the only way to distinguish the origin of the CN bonds observed in a LIBS spectrum. Time evolutions of the band head intensity for CN (at 388.3 nm) and C_2 (at 516.5 nm) bands are shown in Fig. 10 for the four samples: (a) graphite, (b) cellulose nitrate, (c) *E. coli*, and (d) *B. subtilis*. Error bars presented with the data correspond to fluctuations of the signals from one kinetic series to other recorded in the same experimental conditions.

For graphite [Fig. 10(a)], C_2 can be directly released by the sample. The time evolution of its band head intensity is a simple decay from an initial maximal value. However, CN radicals can only be formed by recombination of carbon ablated from the sample and atmospheric nitrogen. The observed increasing band head intensity in the first 472 ns after the laser shot provides the evidence of the recombination of CN radicals. This temporal behavior is clearly distinguished

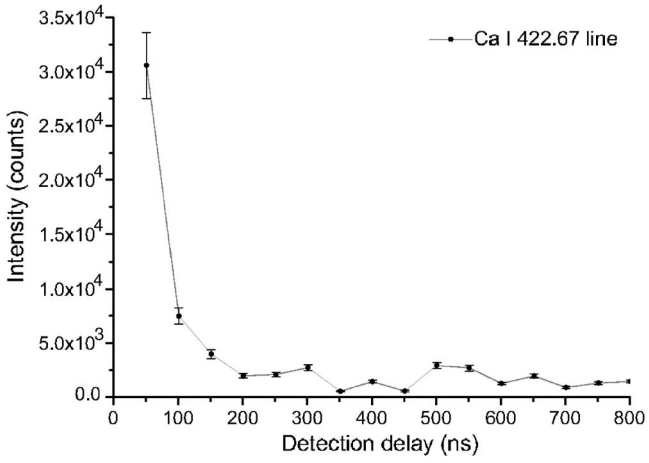

FIG. 9. Time evolution of the Ca I 422.67 line from an *E. coli* sample.

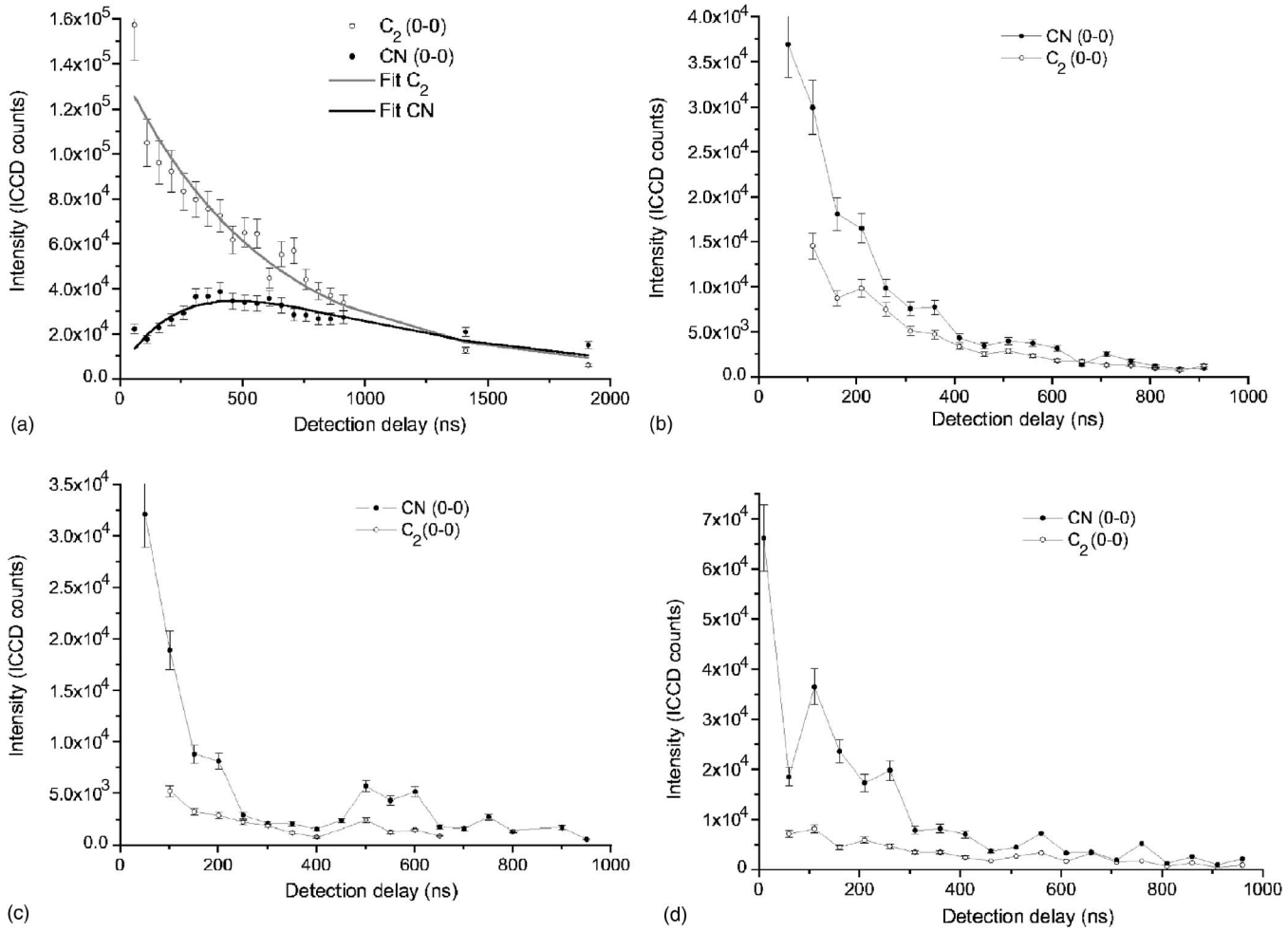

FIG. 10. Time evolutions of band head intensity of CN (at 388.3 nm) and C_2 (at 516.5 nm) for four different samples: (a) graphite, (b) cellulose nitrate, (c) *Escherichia coli*, and (d) *Bacillus subtilis*. The smooth curves in Fig. 10(a) correspond to theoretical fits.

from that of C_2 radicals directly released by the sample. Notice that the observed CN band behaves similarly as what was observed in nanosecond UV ablation of a graphite sample.[21]

For the cellulose nitrate filter [Fig. 10(b)] as well as the two bacterial samples [Figs. 10(c) and 10(d)], a monotonic decreasing behavior is observed for the CN as well as for the C_2 band head intensities. This behavior clearly indicates a different origin of CN radicals as compared to the case of graphite. Using an exponential decay fitting for the CN band head intensities presented in Figs. 10(b)–10(d), and take into account experimental error bars, we get a time constant of 185 ± 45 ns for the filter, 100 ± 30 ns for *E.coli*, and 135 ± 85 ns for *B. subtilis*. Different values in decay time constant are correlated further to the different origins of the observed CN bonds in these two types of sample. For a bacterial sample, CN band can be due to native CN bonds directly ablated from the sample, while for the filter, CN bonds result from an intraplasma recombination between carbon and nitrogen atoms. That suggests a shorter decay time constant of CN bands for a bacterial sample than for an organic carbon- and nitrogen-containing sample. This seems to be confirmed by our experimental data using two different bacteria and an organic sample. One remarks, however, that the difference in CN band decay time constants is not so large compared to the uncertainty due to experimental fluctuations from a kinetic series to other and the difference between two bacteria. Our data from the kinetic study demonstrate thus that the time-resolved femto-LIBS may provide a clear distinction between carbon-containing inorganic or organic samples (for example, graphite, hydrocarbons, etc.) and nitrogen-containing organic or biological samples (especially bacteria). However, a differentiation between a bacterial sample and a nitrogen-containing organic sample using the CN molecular bands requires a more careful quantitative comparison of decay behaviors of the molecular bands. Or other characteristic compounds, such as trace mineral elements, may be used to provide further differentiation.

As already pointed out, when a graphite sample is ablated, CN radicals are mainly formed by gas phase reaction during the propagation of the carbon vapor through the N_2 gas by the reaction: $C_2 + N_2 \leftrightarrow 2CN$.[21] The dynamics of such reaction can be described by the following coupled rate equations:[22]

$$\frac{d[C_2]}{dt} = -k[N_2][C_2] - \upsilon_d^{C_2}[C_2],$$
$$\frac{d[CN]}{dt} = 2k[N_2][C_2] - \upsilon_d^{CN}[CN], \quad (1)$$

where $[x]$ refers the concentration of the species x, k the rate of the reaction, $\upsilon_d^{C_2}$ and υ_d^{CN} the diffusion frequencies for C_2 and CN related to the expansion of the plasma. The solutions of these equations,

$$[C_2](t) = [C_2]_0 e^{-(k[N_2]+\upsilon_d^{C_2})t},$$
$$[CN](t) = \frac{2[C_2]_0}{\upsilon_d^{CN} - (\upsilon_d^{C_2} + k[N_2])}(e^{-\upsilon_d^{CN}t} - e^{-(k[N_2]+\upsilon_d^{C_2})t}), \quad (2)$$

were used to fit the experimental data in Fig. 10(a). A genetic algorithm has been used to adjust the four independent parameters, $[C_2]_0$, $k[N_2]$, $\upsilon_d^{C_2}$, and υ_d^{CN} in order to fit Eq. (2) to the experimental data presented in Fig. 10(a) (a baseline is determined using the signal at a very long detection time). The results show values of 6.58×10^5 s^{-1}, 1.04×10^6 s^{-1}, and 2.60×10^6 s^{-1} for $k[N_2]$, $\upsilon_d^{C_2}$, and υ_d^{CN}, respectively. This value of $k[N_2]$ can be compared to that extracted from the infrared nanosecond regime.[22] We find here a three-time larger value in the femtosecond regime, which implies a lager reaction rate between atmospheric N_2 and C_2 in a lower temperature carbon plasma induced by a femtosecond pulse. We remark also that the value of υ_d^{CN} is significantly larger than that of $\upsilon_d^{C_2}$, which is consistent with the mechanism of recombination between carbon molecules and atmospheric nitrogen molecule in the interface of plasma plume with ambient air. So the population of CN bonds is distributed on the surface of the plasma plume, while that of C_2 is contained in the volume of the plasma.

IV. CONCLUSION

In conclusion, we have demonstrated LIBS analysis of bacteria with femtosecond laser pulses. A comparison between femto and nano-LIBS in the near infrared region demonstrates attractive features related to the use of ultrashort pulses for the LIBS analysis of a biological sample. These attractive features are related to the lower and faster decaying temperature of the femtosecond laser-induced plasma. We have demonstrated thus less interference with emissions from ambient air and higher contrast for the detection of trace elements in a bacterial sample with femto-LIBS. We have also observed a higher ratio between molecular and atomic emissions implying a large concentration of molecular fragments in femtosecond laser-induced plasma. We have shown in particular that native CN bonds released by a bacterial sample can be characterized by a short decay time of its band head intensity. This allows an unambiguous distinction with respect to CN radicals formed by recombination with atmospheric nitrogen, which can be commonly observed in a carbon-containing nonbiological sample (for example, graphite, hydrocarbons, etc.).The strong emission of the CN bands in a femto-LIBS spectrum together with its rapid decay behavior provides a quick, certainly not definitive, indication of a bacterial sample, some kinds of first warning that triggers other more detailed and more sophisticated analysis. Such detailed analysis can be provided by trace mineral elements from a bacterial sample, which can be detected with a high sensitivity using femto-LIBS. These trace elements should contribute to the characterization of a specific bacterium, since they participate in the metabolism of the bacterium and influence their structure. Molecular and atomic spectra thus provide together valuable data for a specific bacterium to be either detected from a natural environment or distinguished from other biological species.

[1] A. C. Samuels, F. C. De Lucia, Jr., K. L. McNesby, and A. W. Miziolek, Appl. Opt. **42**, 6205 (2003).
[2] S. Morel, N. Leon, P. Adam, and J. Amouroux, Appl. Opt. **42**, 6184 (2003).
[3] N. Leone, G. D'Arthur, and P. Adam, High Tech. Plasma Process **8**, 1 (2004).
[4] C. A. Munson, F. C. De Lucia, Jr., T. Piehler, K.L. McNesby, and A. W. Miziolek, Spectrochim. Acta, Part B **60**, 1217 (2005).
[5] A. R. Boyain-Goitia, D. C. S. Beddows, B. C. Griffiths, and H. H. Telle, Appl. Opt. **42**, 6119 (2003).
[6] P. B. Dixon and D. W. Hahn, Anal. Chem. **77**, 631 (2005).
[7] D. C. S. Beddows and H. H. Telle, Spectrochim. Acta, Part B **60**, 1040 (2005).
[8] Ph. Rohwetter, K. Stelmaszczyk, G. Méjean, J. Yu, E. Salmon, J. Kasparian, J.-P. Wolf, and L. Wöste, J. Anal. At. Spectrom. **19**, 437 (2004).
[9] K. Stelmaszczyk *et al.*, Appl. Phys. Lett. **85**, 3977 (2004).
[10] Ph. Rohwetter *et al.*, Spectrochim. Acta, Part B **60**, 1025 (2005).
[11] See, for example, Proceedings of the Fifth International Conference on Laser Ablation, edited by J. S. Horwitz, H.-U. Krebs, K. Murakami, and M. Stuke, in [Appl. Phys. A: Mater. Sci. Process. **69** (1999)].
[12] B. Le Drogoff *et al.*, Spectrochim. Acta, Part B **56**, 987 (2001).
[13] B. Le Drogoff, J. Margot, F. Vidal, M. Chaker, M. Sabsabi, T. W. Johnston, and O. Barthélemy, Plasma Sources Sci. Technol. **13**, 223 (2004).
[14] X. Zeng, X. Mao, R. Greif, and R. E. Russo, Proc. SPIE **5448**, 1150 (2004).
[15] S. S. Mao, X. Mao, R. Greif, and R. E. Russo, Appl. Phys. Lett. **77**, 2464 (2000).
[16] G. J. Basttiaan and R. A. Mangold, Spectrochim. Acta, Part B **40**, 885 (1985).
[17] T. Lipper, A. Wokaun, S. C. Langford, and J. T. Dickinson, Appl. Phys. A: Mater. Sci. Process. **69**, S655 (1999).
[18] R. Srinivasan and B. Braren, Chem. Rev. (Washington, D.C.) **89**, 1303 (1989).
[19] B. D. Koplitz and J. K. McVey, J. Phys. Chem. **89**, 4196 (1985).
[20] P. Singleton, *Bacteria in Biology, Biotechnology and Medicine*, 4th ed. (Wiley, Chichester, England, 1997).
[21] C. Vivien, J. Hermann, A. Perrone, C. Boulmer-Leborgne, and A. Luches, J. Phys. D **31**, 1263 (1998).
[22] L. St-Onge, R. Sing, S. Béchard, and M. Sabsabi, Appl. Phys. A: Mater. Sci. Process. **69**, S913 (1999).
[23] http://www.physics.nist.gov/PhysRefData/ASD/lines_form.html.
[24] *Tables Internationales de Constantes Sélectionnées*, Données Spectroscopiques Relatives aux Molécules Diatomiques, Vol. 17, B. Masson, ed. (Pergamon, New York, 1970).